NANOPATTERNED SURFACES FOR THE EXPLORATION OF CELL BEHAVIOR

UNDEGRADUATE HONORS RESEARCH THESIS

Presented in Partial Fulfillment of the Requirements for the Bachelor of Science with Honors Research Distinction in the College of Engineering of The Ohio State University

By

Kunal Sailesh Parikh

The Ohio State University

March 2012

Honors Thesis Committee

Dr. Jessica Winter, Advisor
Dr. Sheikh Akbar

Abstract

Surfaces with ordered, nanopatterned roughness have demonstrated considerable promise in directing cell morphology, migration, proliferation, and gene expression. However, further investigation of these phenomena has been limited by the lack of simple, inexpensive methods of nanofabrication. Here, we report a facile, low-cost nanofabrication approach based on self-assembly of a thin-film of gadolinium-doped-ceria on yttria-stabilized zirconia substrates (GDC/YSZ). This approach yields three distinct, randomly-oriented nanofeatures of variable dimensions, similar to those produced via polymer demixing, which can be reproducibly fabricated over tens to hundreds of microns. As a proof-of-concept, we examined the response of SK-N-SH neuroblastoma cells to features produced by this system, and observed significant changes in cell spreading, circularity, and cytoskeletal protein distribution. Additionally, we show that these features can be imprinted into commonly used rigid hydrogel biomaterials, demonstrating the potential broad applicability of this approach. Thus, GDC/YSZ substrates offer an efficient, economical alternative to lithographic methods for investigating cell response to randomly-oriented nanotopographical features.

Acknowledgments

There a number of individuals who have contributed both to this work and to my personal growth and development. I have been incredibly fortunate to have had the privilege to work with and learn from them, and mere words cannot express my gratitude.

First and foremost, I would like to acknowledge the continued guidance and support of Dr. Jessica Winter, without whom this work would not be possible. I am also forever indebted to Dr. Gregory Washington and Dr. David Tomasko who encouraged and provided me with the opportunity to begin research as a high school senior, and have served as valuable mentors since.

I would also like to thank Dr. Sheikh Akbar, Dr. Burr Zimmerman, and Haris Ansari, who first introduced me to nanopatterned materials, and have served as tremendous collaborators and partners in innovation. I am also grateful to Dr. Jed Johnson, Shreyas Rao, and Dhananjay Thakur for serving as mentors, friends, and invaluable resources over the past few years.

Financial support for this work was received from The Ohio State University, the Center for Affordable Nanoengineering of Polymeric Biomedical Devices (CANPBD), the Nanoscale Science and Engineering Center (NSEC), and the H.C. “Slip” Slider Professorship to Dr. Jessica Winter.

Finally, I would like to thank Sailesh, Sonal, and Paras Parikh whose unwavering support and sacrifice compel me to take advantage of every opportunity I am given and strive to better the world around me.

VITA

July 19, 1990 . . . . . Born – Reynoldsburg, Ohio

2008-2012 . . . . . Undergraduate Research Assistant,
The Ohio State University

2010 . . . . . Honors & Scholars Summer
Research Fellowship,
The Ohio State University

2010-2012 . . . . . Undergraduate Research Scholar,
The Ohio State University

2012 . . . . . 3rd Place Denman Undergraduate
Research Forum,
The Ohio State University

2012 . . . . . B.S. Chemical Engineering,
The Ohio State University

PUBLICATIONS

1. J. O. Winter, N. Han, M. Owens, J. Larison, J. Wheasler, K. Parikh, L. Siers. "Polymer Hydrogel Thin Film Coatings for Acute Drug Delivery from Neural Prostheses." *PMSE Preprints*, 99:801-802. (2008).

2. N. Han, S. S. Rao, J. Johnson, K. Parikh, P. Bradley, J.J. Lannutti, J.O. Winter. "Hydrogel-Electrospun Fiber Mat Composite Coatings for Neural Prostheses." *Frontiers in Neuroengineering.* (2011).

FIELDS OF STUDY

Major Field: Chemical Engineering

Minor Fields: Entrepreneurship, Political Science

Table of Contents

List of Figures

List of Tables

1. Introduction

A key aspect of tissue engineering and especially biomaterial applications is the manufacture of surfaces to induce or enhance *in vivo* cell behavior under *in vitro* conditions. In order to achieve this objective, novel systems have been designed to provide bioactive surfaces to cells. These systems utilize several methods of manipulation, including the use of chemical signaling, surface proteins, mechanical forces, electrical fields, and substrate topography (1). Currently, scientists are determining the effects of each individual cue to more fully understand and refine these mechanisms in the manipulation of cell behavior.

Substrate topography, especially on the nanoscale, is considered a promising tool for the manipulation of cells in tissue scaffolds. Although the influence of surface topography on cell response was first identified nearly 100 years ago (2), a detailed understanding of the mechanisms by which cells respond to their physical environment, particularly on the nanoscale, has yet to be achieved. This understanding is important not only because nanoscale features could be used to guide cell behavior, but also because many biomaterials exhibit nanoscale roughness, which may unintentionally guide cell response. Cells interact with biomaterials by adhering to the substrate through the formation of focal contacts and the development of a defined cytoskeleton. This in turn affects cell differentiation, proliferation, spreading, and signal transduction pathways, all of which are integral in determining cell response to the external environment.

Nanotopography has been shown to increase cell adhesion and migration, and to alter cell orientation, gene expression, contact inhibition, and cytoskeletal structure (1-4). Thus, tremendous opportunities lie in the application of a controlled nanoenvironment to elicit a certain cell response. However, prior to the application of nanotopography to biomaterials, it is necessary to fully explore the relationships between pattern type, pattern dimension, and cell type, requiring a myriad of additional experiments.

The most common approaches to fabrication of materials for investigation of cell response to nanopatterns are derived from the semiconductor industry (5). These methods include photolithography, electron beam lithography, and interference lithography, which are capable of producing ordered, reproducible features over substrates on the order of mm x mm in size (6-8). However, these techniques can be time consuming and require access to expensive equipment. In contrast, less expensive, facile methods of nanofabrication have been developed, such as electrospinning, chemical etching, polymer demixing, and colloidal lithography; however, control of feature geometry can be challenging, especially over large substrate areas (4, 7). These disadvantages characteristic of current systems of nanofabrication simply make it unfeasible and/or futile to complete the multitude of experiments necessary to fully elucidate cell response to nanofeatures, and utilize this knowledge in the creation of biomaterials. A model system of nanofabrication for investigating the effects of nanotopography on cell function must provide for the manufacture of a pattern that is inexpensive, reproducible, scalable, high throughput, able to be manufactured on biocompatible materials, and time efficient. Here, we demonstrate a novel nanofabrication method to explore the effects of nanotopography on cell behavior based on self-assembled ceramic surfaces (9). This

system consists of an yttria-stabilized zirconia (YSZ) substrate, coated with a thin film of gadolinium-doped ceria (GDC, through RF magnetron sputtering), which is then annealed. Pseudo-periodic nanofeatures, consisting of YSZ and GDC, are spontaneously produced as a result of a morphological instability in lattice mismatched thin films, which causes the surface to reorder by diffusion to relieve stress (9, 10). Variation in annealing temperature, duration, or GDC film thickness allows three types of arrayed nanopatterns to be created: islands, connected islands, and pits. This system is scalable, with useable substrate size primarily limited by the size of the furnace and YSZ substrate employed, and is also highly controllable, with great flexibility to vary height, length, and depth, and thus provides an alternative method of nanofabrication for investigating cell response to nanofeatures.

To demonstrate proof of concept, we examined the effect of surface topography in the form of 36 nm islands, 56 nm connected islands, and 37 nm deep pits manufactured by the GDC/YSZ system on cell morphology, circularity, spreading, and adhesion. Additionally, we examined focal contact formation by evaluating actin, vinculin, and integrin expression *in vitro*. As a model system, we utilized SK-N-SH neuroblastoma cells as these cells are known to change morphology in response to external stimuli (11). These studies demonstrate the potential of the GDC/YSZ system to explore cell response to nanotopography. Further, we show that GDC/YSZ substrates can be imprinted into commonly used biomaterials (e.g., ethylene dimethacrylate (EGDMA) hydrogels), which would permit this approach to be widely adopted.

2. Materials and Methods

2.1 Fabrication of nanopatterned surfaces

Manufacture of the GDC target, GDC sputtering, and production of nanopatterned surfaces were performed as described previously (10). Briefly, GDC sputtering was achieved utilizing a Discovery 18 DC/RF magnetron sputter deposition system (Denton Vacuum, Moorestown, NJ). A 7.62 cm diameter and 3.2 mm thickness GDC target (stoichiometric composition: $Ce_{0.89}Gd_{0.11}O_{1.95}$; nominal specific surface area: 35–47 m^2 g^{-1}) (Nextech Materials, Columbus, OH), sintered at 1350^{o}C to a density of 5.18 $g \cdot cm^{-3}$ (71.1% theoretical) and mounted in a copper backing cup (Sputtering Target Manufacturing Co., LLC, Westerville, OH) was employed. A 1.5 nm film was produced by sputtering at 60 W for 1 minute in an argon gas environment of 5 mTorr on single crystal 8 mol% 5.0 × 5.0 × 0.5 mm YSZ substrates with (100) surface orientation chemically polished to a 5 Å surface roughness (MTI Corporation, Richmond, CA). Films of 3 and 4.5 nm thicknesses were produced by sputtering at 60 W and 5 mTorr for 2 and 3 minutes, respectively. Island and connected island morphologies were obtained by annealing 1.5 and 4.5 nm film substrates, respectively, in a tube furnace (Blue M model #TF55035A, Lindberg, Riverside, MI) for 10 hours at 1100^{o}C. Pits were formed by annealing 3 nm film samples for 1 hour at 1300^{o}C in a box furnace (Lindberg 1500^{o}C, model# BF51433PBC). YSZ substrates with a 1.5 nm GDC film were utilized as a control. All experimental substrates were sonicated for 15 minutes in acetone (Sigma-Aldrich, St. Louis, MO), washed in distilled, deionized (DI) water, and autoclaved for

sterilization prior to use in cell studies. Surfaces were characterized using atomic force microscopy (AFM, MFP-3D-Bio atomic force microscope, Asylum Research, Santa Barbara, CA) and scanning electron microscopy (SEM, Sirion, FEI Company, Hillsboro, OR). SEM Samples were osmium coated to a thickness of 15 nm (Osmium Plasma Coater, Structure Probe, Inc., West Chester, PA) or gold coated (Model 3 Sputter Coater 91000, Pelco, Reading, CA) for 1 minute prior to imaging at an acceleration voltage of 12 kV.

2.2 Large scale nanofabrication

A 3 nm film of GDC was sputtered onto a single crystal 8 mol% 25.4 × 25.4 × 0.5 mm YSZ substrate with (100) surface orientation chemically polished to a 5 Å surface roughness (MTI Corporation) at 60 W for 2 minutes in an argon gas environment of 5 mTorr. The sample was then annealed for 1 hour at 1300^{0}C in a box furnace as described above to form pits. The sample was then cut into 9 separate quadrants. The four corner quadrants and middle quadrant were imaged via SEM to determine scalability and reproducibility. Fast Fourier transform (FFT) analysis was performed on opposite corners using Image J image analysis software (http://rsbweb.nih.gov/ij) to determine the periodicity and uniformity of nanofeatures across the substrate.

2.3 Contact angle and surface energy measurements

Experimental and control surfaces were characterized by contact angle and surface energy measurements performed using an EasyDrop DSA20 system (KRÜSS, Hamburg, Germany) by dropping a bead of water onto each surface and subsequently measuring contact angle (N=4).

Surface energy was determined through the equation of state (12):

$$\cos\theta = -1 + 2\sqrt{\frac{\sigma_s}{\sigma_l}}e^{-\beta(\sigma_l-\sigma_s)^2} \qquad (1)$$

where θ is the contact angle obtained by measurement, σ_s is the surface tension of the solid, σ_l is the surface tension of the liquid drop (water = 0.0742 N/m, experimentally determined), and β is a constant equal to 0.0001247 (13). Contact angle measurements were performed at 23.9ºC at 50% relative humidity.

2.4 SK-N-SH cell culture and quantification of cell spreading and morphology

SK-N-SH neuroblastoma cells (American Type Culture Collection, Manassas, VA) were cultured at 37^{o}C in a 5% CO_2 atmosphere in Dulbecco's Minimal Essential Medium (Sigma-Aldrich) supplemented with 10% fetal bovine serum (Sigma-Aldrich), and 1% penicillin/streptomycin (Invitrogen, Carlsbad, CA). Cells were fed 2-3 times a week and passaged weekly at confluence prior to use. Cells were seeded at 1 x 10^4 cells/ml in complete medium on each substrate and incubated for 24 hours. Cells were washed in phosphate buffered saline (PBS, Sigma-Aldrich) and fixed in 4% paraformaldehyde (Sigma-Aldrich) buffered in Dulbecco's PBS (D-PBS, Sigma-Aldrich) with sucrose and sodium chloride. Cells were then dehydrated through a series of alcohol concentrations in DI water (12.5, 25, 50, 75, 90, 100% ethanol) (Sigma-Aldrich), osmium coated, and imaged by SEM at 12 kV, utilizing the backscatter electron detector. Cell properties (e.g., area, circularity) were quantified utilizing NIH Image J image analysis software. Cell area and circularity were measured by randomly selecting four sections of each sample and measuring individual cell areas and circularities (n=10) in each section.

2.5 Focal contact labeling

Cells were seeded on experimental substrates at 1 x 10^4 cells/ml in complete medium and incubated for 24 hours prior to fixation with 4% paraformaldehyde for 20 minutes. Cells (N=3) were then washed with D-PBS and extracted with 0.1% Triton X-100 (Sigma-Aldrich) for actin and vinculin labeling. Cells were washed with D-PBS and then blocked using a solution of 1% bovine serum albumin (Sigma-Aldrich) in D-PBS at 4^{o}C for 1 hour for vitronectin and vinculin staining, and 30 min for actin labeling. Cells were washed with D-PBS, and Alexa Fluor 633 (Phalloidin) (Molecular Probes, Inc, Eugene, OR), anti-vinculin primary antibody (diluted 1:100 in 1% BSA/D-PBS; Accurate Chemical and Scientific Corporation, Westbury, NY), or anti-vitronectin primary antibody (diluted 1:50 in 1% BSA/DPBS; Jackson ImmunoResearch Laboratories, Inc, Wet Grove, PA) were added for actin, vinculin, and vitronectin labeling, respectively. Actin-labeled cells were incubated at room temperature for 20 minutes, whereas vinculin and vitronectin labeled cells were incubated at 4^{o}C for 30 minutes. Cells were then washed with D-PBS and the secondary antibody (diluted 1:50 in 1% BSA/D-PBS; Jackson ImmunoResearch) was added to both vinculin and vitronectin labeled cells, which were incubated at 4^{o}C for 30 minutes. After washing in D-PBS, *Slow*Fade Gold (Molecular Probes, Inc) was added to each sample to preserve fluorescence. Substrates were placed face down, and imaged at 100X magnification using an Inverted Microscope (IX71, Olympus, Melville, NY) equipped with fluorescence filters.

2.6 Nanoimprinting on hydrogel surfaces

Connected island substrates were produced as described above and gold coated for 1 minute. Samples were then soaked in 1 ml of 1-octanethiol (Sigma-Aldrich) for 2 hours.

An 8-well SecureSeal hybridization chamber (Grace Bio-Labs, Bend, Oregon) was then placed on a glass microscope slide treated with piranha solution (1:1 70% H_2SO_4:30% H_2O_2). Experimental samples (N=4) were placed face-up in the well, which was then filled with a 1 wt% solution of Irgacure 651 initiator in EGDMA (98%, Sigma-Aldrich). Another piranha treated glass microscope slide was then placed above the solution, which was cured by UV light for 15 minutes under argon as described previously (10). Cured EGDMA was separated from the sample and dehydrated with a graded series of ethanol solutions in DI water (50, 70, 80, 95, and 100% ethanol) followed by graded solutions of hexamethyldisilazane (HMDS, Sigma-Aldrich) in ethanol (25, 50, 75, and 100% HMDS) for imaging. Dehydrated EGDMA samples were then gold coated for 1 minute and observed using SEM.

2.7 Statistical analysis

Cell spreading and circularity data were analyzed by analysis of variance (ANOVA) using JMP statistical software (Version 9). Means were compared using a Tukey-Kramer HSD test to determine significance at an alpha value of 0.05.

3. Results

3.1 GDC/YSZ substrate synthesis and characterization

GDC thin films were sputter-coated onto YSZ substrates and annealed in a furnace. This resulted in thin films with nanopatterned features produced via a morphological instability in lattice mismatched GDC thin film on YSZ substrates that causes the surface to reorder by diffusion to relieve stress (9, 10). Topographical dimensions depended on sputtering and annealing conditions, and AFM and SEM images revealed three distinct, reproducible nanofeatures: islands (Figures 1a, 2a), connected islands (Figure 1b, 2b), and pits (Figure 1c, 2c). Both islands and connected islands exhibited positive features, whereas pits exhibited negative features. Connected islands were larger than islands, displaying both greater height and feature area, whereas pits were similar in depth to islands and in feature area to connected islands (Table 1). Pits also exhibited greater feature spacing, nearly double that of islands and connected islands, which were similar (Table 1). The GDC/YSZ system is capable of producing features between 75 and 250 nm in width and 100 to 2500 nm in length. Features are uniform over the majority of the substrate (Figures 3), with edge effects apparent on the outer 2-4% of each substrate (Figure 4).

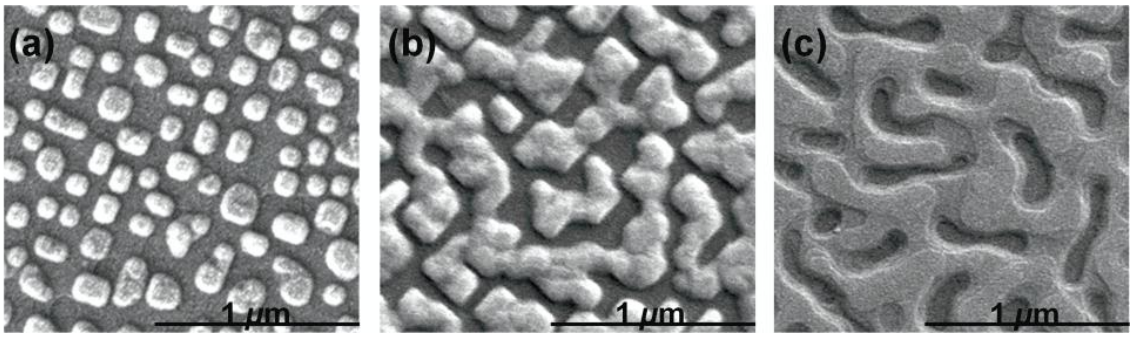

Figure 1. Scanning electron microscopy (SEM) of nanofeatures manufactured using the GDC/YSZ system: (a) islands, (b) connected islands, and (c) pits.

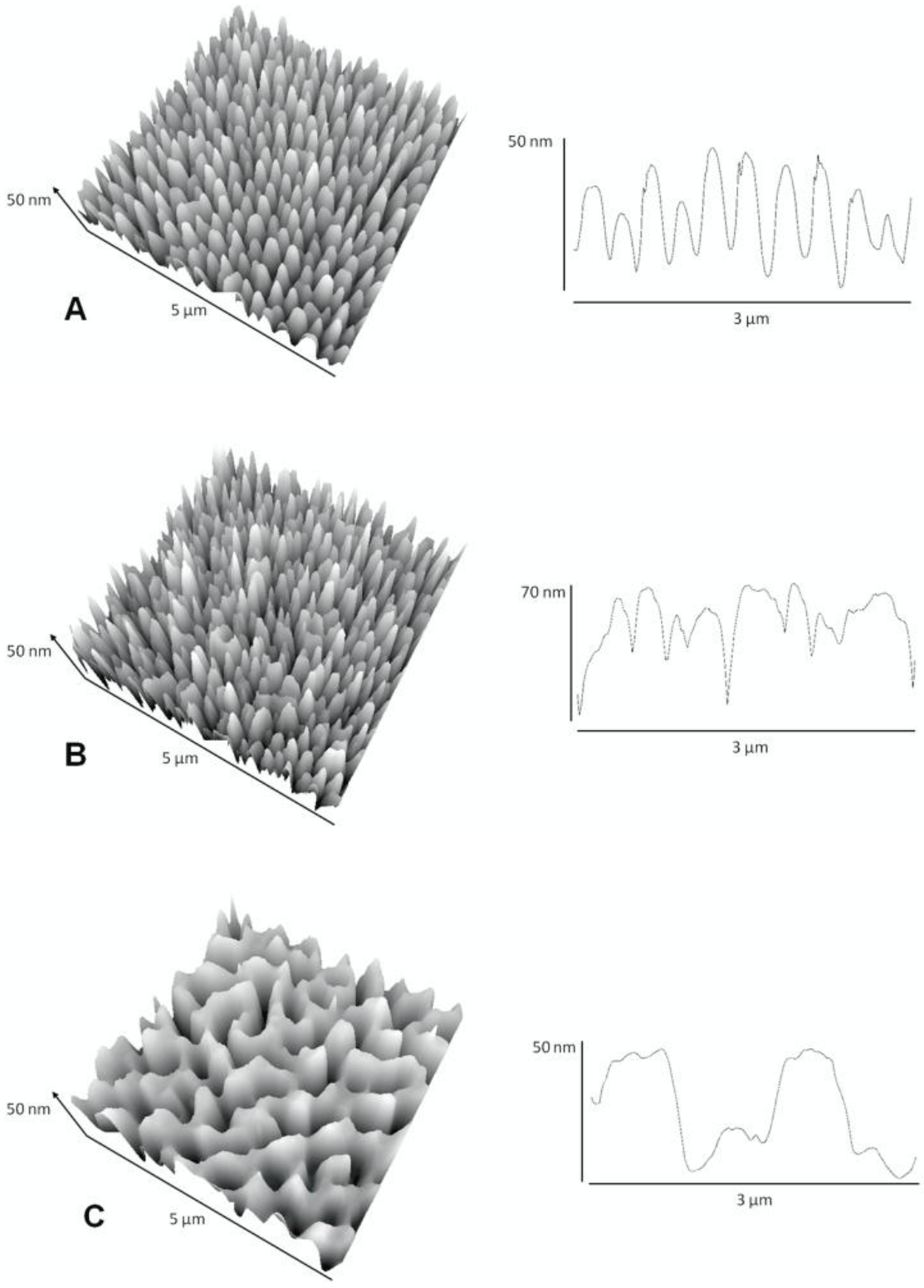

Figure 2. Atomic force microscopy (AFM) of: (a) islands, (b) connected islands, and (c) pits.

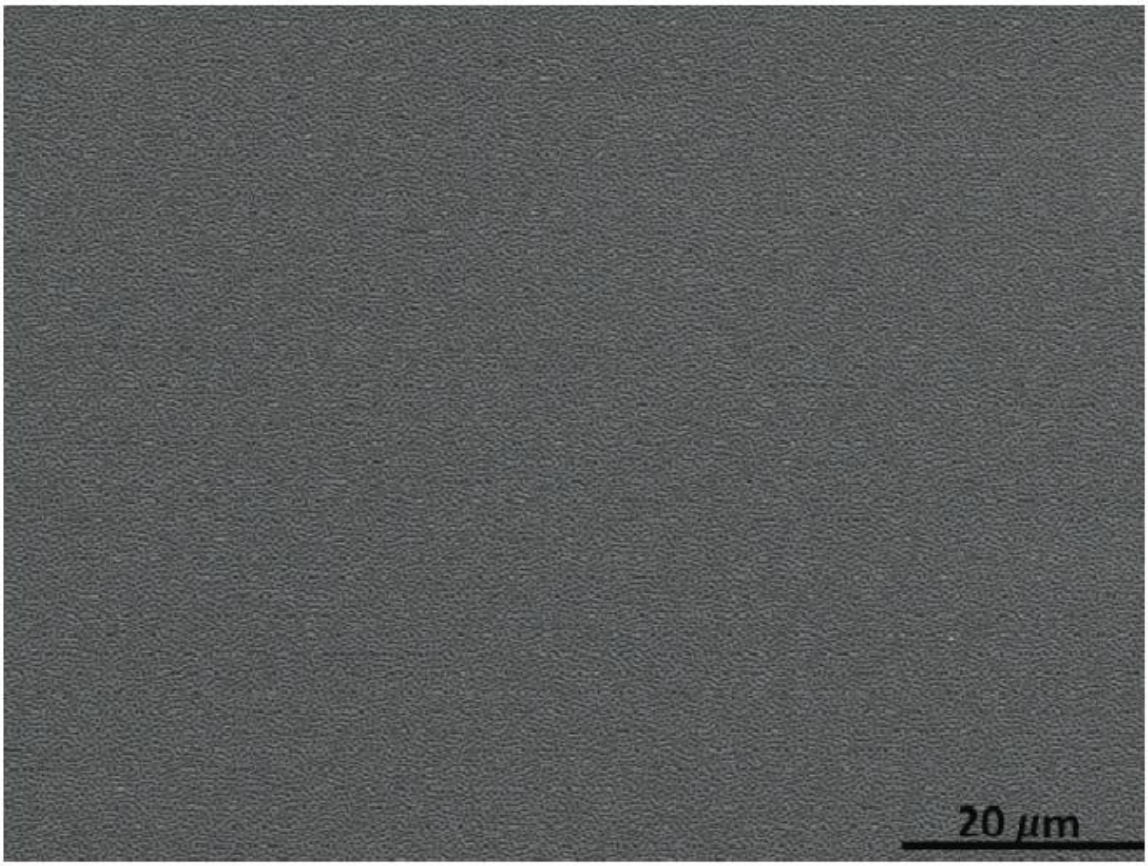

Figure 3. Scanning electron microscopy (SEM) of a 25.4 mm GDC-YSZ pit substrate. Uniform pits shown in the image span an area of 6,300 μm^2.

Table 1. Feature Dimensions and Spacing

Substrate	Average Feature Height (nm)	Average Feature Area (nm^2)	Average Feature Spacing (nm)
Islands	36.0 ± 1.54	16200 ± 8010	55.3 ± 35.0
Connected Islands	56.9 ± 1.84	115000 ± 99000	65.7 ± 33.5
Pits	36.6 ± 2.13	94900 ± 77200	124 ± 53.5

Features manufactured with the GDC/YSZ system are reproducible and can be scaled to the YSZ substrate size assuming that temperature can be maintained constant across the substrate during annealing.

To demonstrate the scale over which uniform features can be achieved, nanofeatures (e.g., pits) were patterned across a 25.4 mm YSZ substrate. Images of the opposing substrate corners (Figure 4) demonstrate the remarkable uniformity of this process, which was further confirmed via Fast Fourier Transform (FFT) analysis. Excluding edge effects (i.e., the outer ~1 mm of the chip), pits were uniformly produced across a diagonal span of 33 mm or a total area of 548 mm^2 (e.g., Figure 3). Thus, the GDC/YSZ system can be used to produce reproducible features over large scales, providing nanofeatures through unprecedented ease and with uniformity over mm length scales.

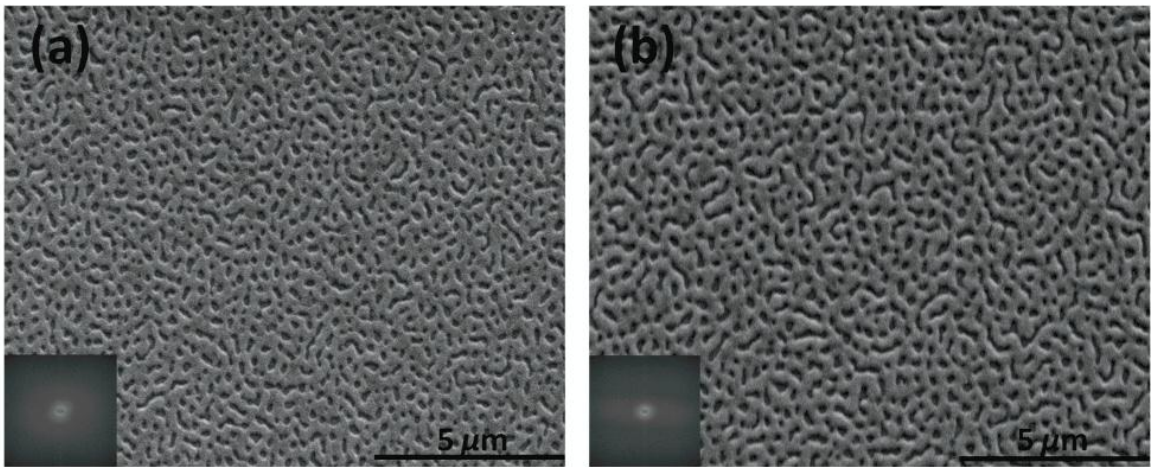

Figure 4. SEM of opposite corners of a 25.4 mm GDC/YSZ pits substrate: (a) substrate top-right and (b) bottom-left. Inset shows Fast Fourier Transform (FFT) analysis of the pictured surfaces.

Substrates were further characterized using contact angle and surface energy measurements (Table 2) to determine wettability, which can directly influence cell behavior. Each of the three nanofeatures and a smooth GDC on YSZ control film were analyzed. The smooth control is slightly hydrophobic, whereas patterned surfaces are hydrophilic, with islands and connected islands having similar contact angle and surface

energy measurements. Nanopatterned surfaces most likely display lower contact angles because of surface roughness, and enhanced wettability due to increased surface area (14).

Table 2. Contact angle and surface energy of GDC/YSZ experimental surfaces.

Substrate	Contact Angle (°)	Surface Energy (mN/m)
Smooth Control	106	19.54
Islands	64.6	45.01
Connected Islands	69.0	42.34
Pits	84.4	32.73

3.2 Cell response to nanopatterned GDC/YSZ features

To evaluate the utility of the GDC/YSZ system in evaluating cell response, we investigated the behavior of SK-N-SH neuroblastoma cells on the three nanofeature substrates (i.e., islands, connected islands, and pits) and compared these to a smooth surface control consisting of a thin (i.e., 1.5 nm) GDC film on YSZ. SK-N-SH cells were selected because they are known to alter their morphology in response to environmental factors, such as seeding density, and are therefore expected to be sensitive to nanofeatures (11).

3.2.1 Cell morphology on GDC/YSZ substrates

SK-N-SH neuroblastoma cells reveal distinct phenotypes dependent upon nanofeature morphology (Figures 5, 6). The smooth control induced a flat, polarized, spread morphology (Figures 5a, 6a) similar to neuroblastoma cells on tissue culture polystyrene. In contrast, cells cultured on nanoislands showed a rounded morphology (Figures 5b, 6b), whereas cells on both connected islands (Figures 5c, 6c) and pits (Figures 5d, 6d) exhibited increased cell length and polarity compared to smooth surface controls.

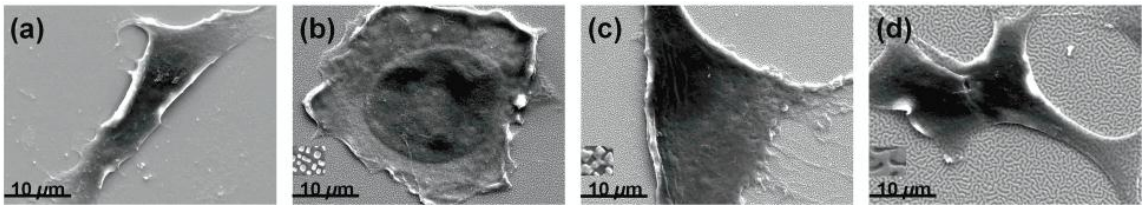

Figure 5. SEM of morphology of representative single SK-N-SH cells on the (a) smooth control, (b) islands, (c) connected islands, and (d) pits. In some cases, nanofeatures can be viewed in the image background. These are also shown in the enlarged insets above the scale bar.

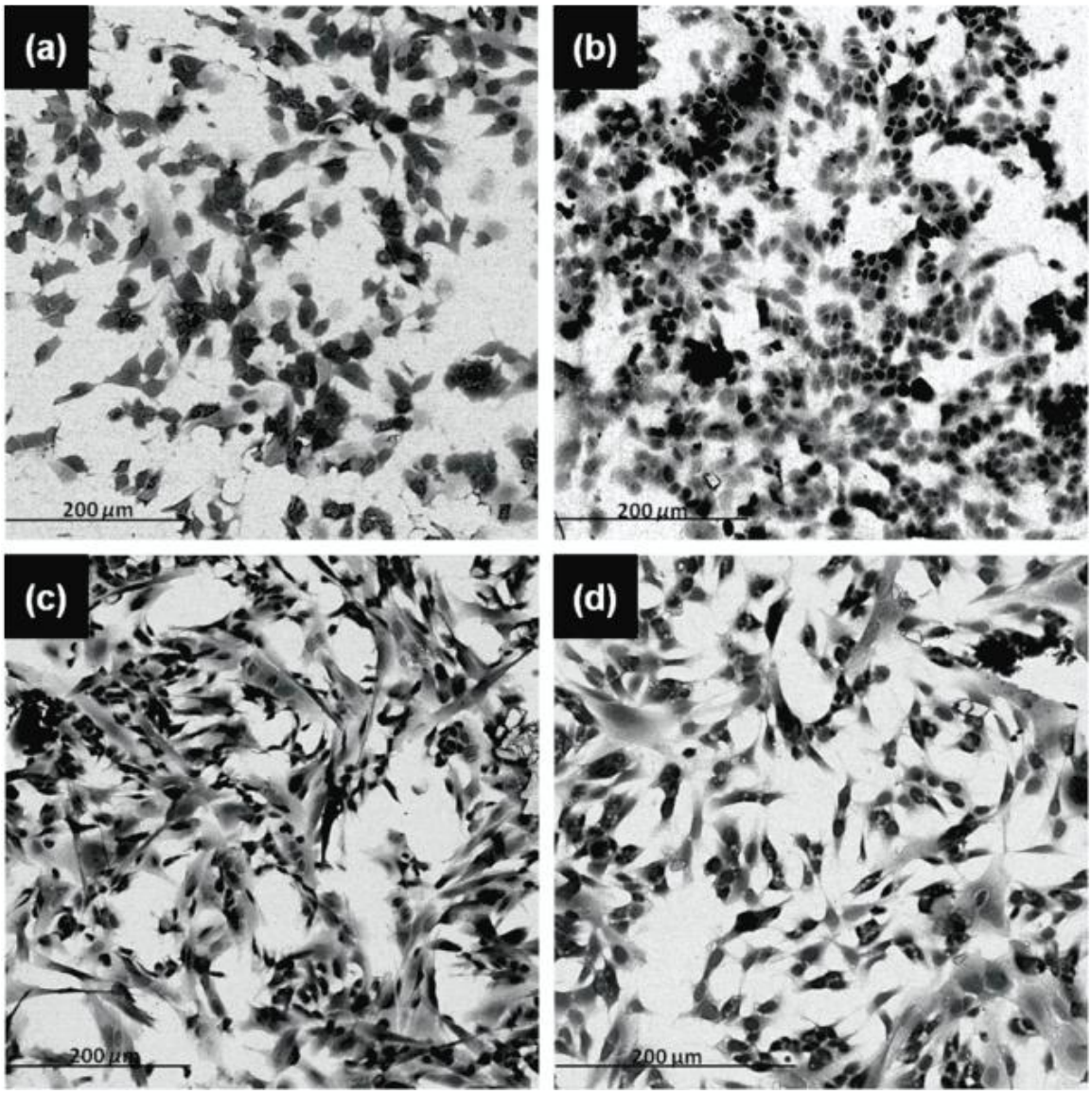

Figure 6. SEM (using a backscattered electron detector) images of the morphology of SK-N-SH cell colonies on (a) smooth control, (b) islands, (c) connected islands, and (d) pits surfaces.

SK-N-SH cell morphology was further examined using NIH Image J image analysis software to quantify cell area and circularity. Cell area on connected island surfaces was significantly greater ($p = 0.0006$) and nearly double that displayed on all other surfaces (i.e., ~750 μm^2 for connected islands vs. ~280 – 400 μm^2 for other surfaces) (Figure 7a). Cell circularity analysis confirmed visual observations that cells grown on islands were significantly more rounded than cells grown on smooth control, connected island, or pit surfaces (Figure 7b). Further, cells grown on the smooth control were also significantly more rounded than cells on connected islands or pits. Thus, cells displayed polarized morphologies indicative of strong attachment on both connected islands and pits, but exhibited significant spreading only on connected island surfaces.

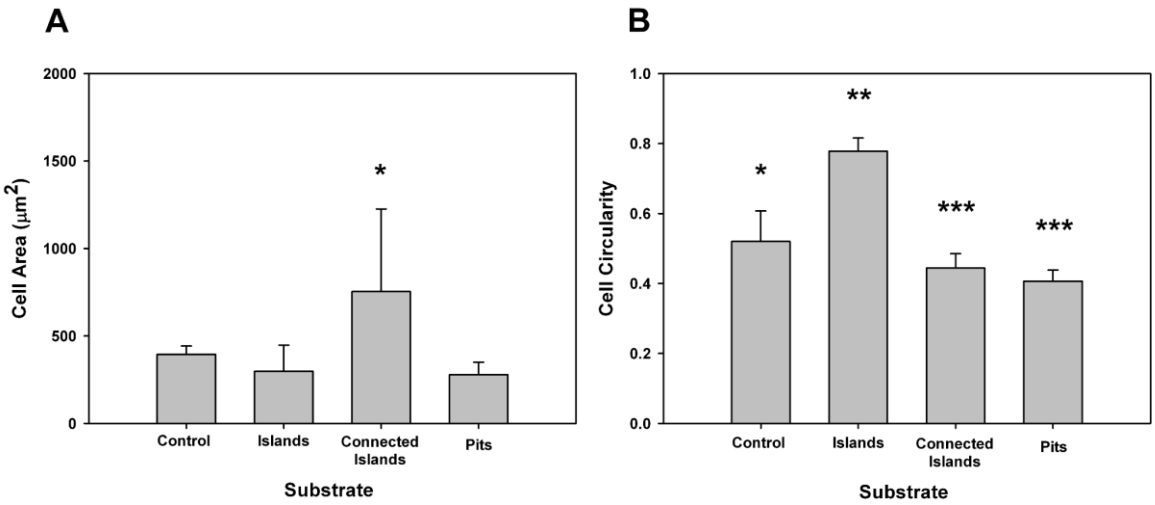

Figure 7. (a) SK-N-SH cell spreading area and (b) circularity on islands, connected islands, pits, and the smooth control substrates. Samples that are statistically significant from each other utilizing a p-value of 0.05 are marked by a different number of stars.

3.2.2 Focal contact formation on GDC/YSZ substrates

To further investigate the influence of nanotopography on underlying focal contact structures, immunochemical labeling of the actin cytoskeleton, vinculin accessory proteins, and vitronectin integrins was performed (Figure 8). Actin expression varied depending on nanofeature morphology. Cells seeded on connected islands displayed mature, elongated stress fibers, consistent with cell spreading and circularity measurements. Cells grown on pits, which also displayed a polarized morphology, and the smooth control, contained fibers concentrated towards the periphery of the cell. In contrast, cells grown on islands did not exhibit developed fibers, as would be expected given their observed rounded and poorly spread morphology.

Vinculin, an actin accessory protein, is also expressed by cells cultured on these substrates, clearly outlining the nucleus. However, labeling is more localized on connected islands, which display punctate staining throughout the cytoplasm. Vinculin expression, especially within the cell body, indicates the formation of focal contacts, which are exhibited in cells seeded on all surfaces, including islands. The $\alpha_v\beta_3$ cell surface receptor is over-expressed in SK-N-SH neuroblastoma cells and binds the vitronectin extracellular matrix protein, facilitating cell adhesion (15). Vitronectin receptors are clearly distinguished at the cell exterior for all substrates via their punctate staining. The most significant difference between these surfaces is the lack of a defined actin structure within cells grown on islands, whereas vinculin and vitronectin are expressed in all cells regardless of substrate topography. However, the expression of vinculin on the surface of cells seeded on islands coincides only with the region of the cell body containing the resemblance of an actin cytoskeleton. These peripheral clusters most likely allow for the adhesion of these cells to the island surface. In contrast, the

clustered expression of actin, vinculin, and vitronectin in cells grown on the smooth control, connected islands, and pits surfaces, in addition to observed cell spreading, indicates the formation of well-developed focal adhesions. However, cells grown on connected islands appear to have a greater number of focal contacts, in proportion to their greater relative cell size. Focal contacts for control and pits surfaces are primarily located on the periphery of the cell body.

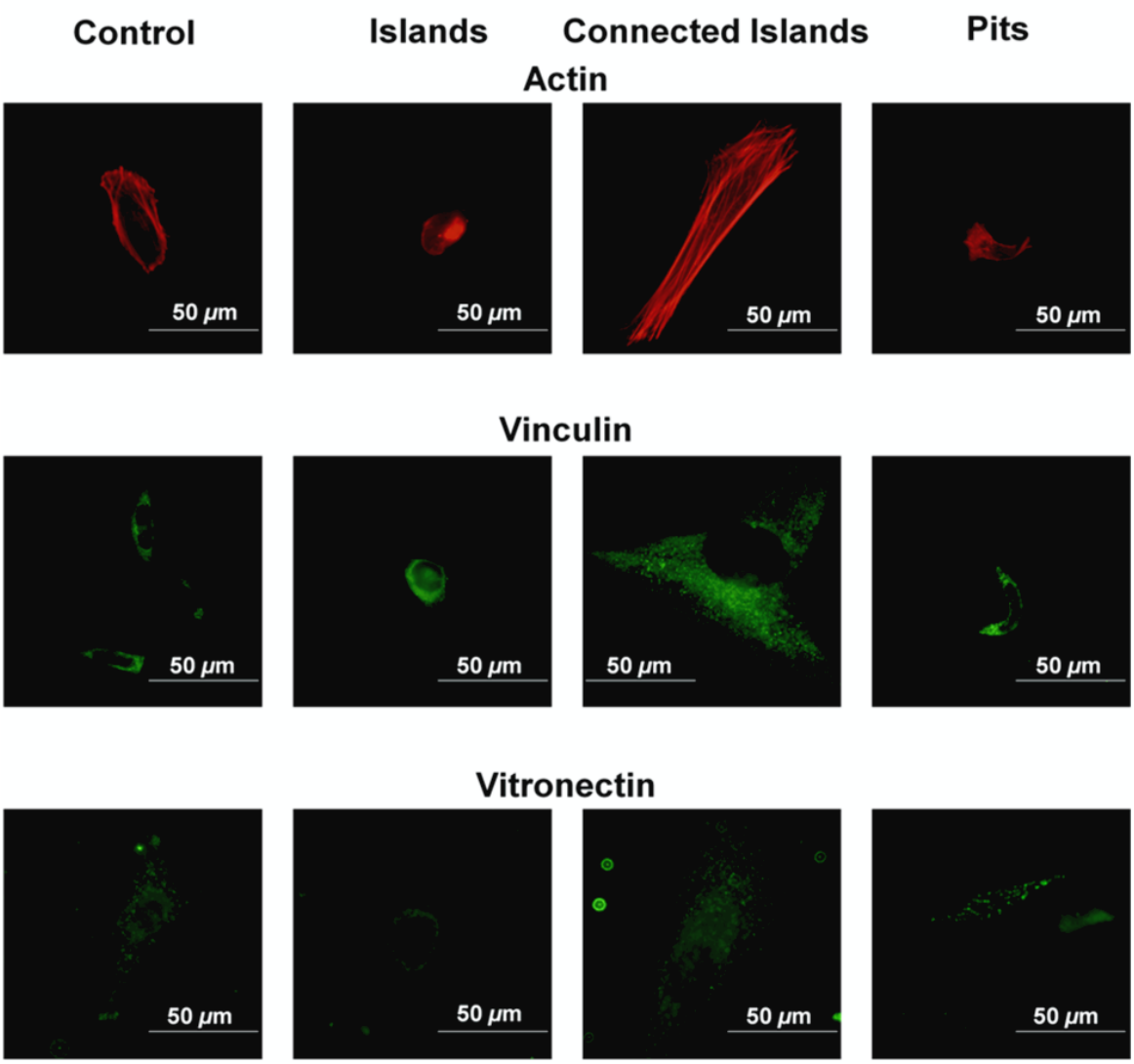

Figure 8. Expression of proteins associated with focal contact formation in SK-N-SH neuroblastoma cells cultured on islands, connected islands, pits, and smooth control surfaces.

3.3 Hydrogel nanoimprinting using the GDC/YSZ system

Although the GDC/YSZ system provides a simple, efficient, cost-effective method to explore cell response to nanotopography, as a ceramic system, it is limited in its ability to mimic biological features and provide biological cues. However, nanofeatures produced by GDC/YSZ substrates can be imprinted into hydrogels (Figure 9) (10), increasing their biological relevance. Hydrogels are crosslinked, hydrated polymer networks that can be adapted to provide chemical and material properties similar to natural tissue (16). In particular, hydrogels composed of poly(ethylene glycol) (PEG) and its derivatives, have been widely used for drug delivery and tissue engineering applications (17, 18). GDC/YSZ nanofeatures (e.g., connected islands) can be imprinted into PEG-based hydrogels (i.e., ethylene glycol dimethacrylate (EGDMA)), and thus could potentially be used to provide nanotopography to this important class of biomaterials.

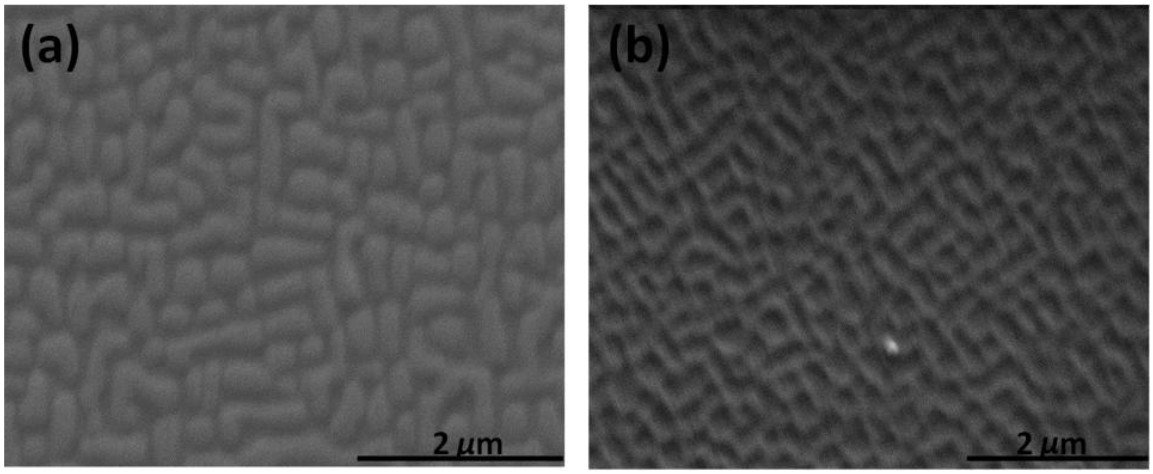

Figure 9. (a) Ceramic connected islands produced using GDC/YSZ ceramics can be imprinted into (b) EGDMA hydrogel.

4. Discussion

Here, we demonstrate a low cost approach for creating a variety of nanofeatures over large surface areas, which could be used to examine the influence of cell response to nanotopography. This nanomanufacturing method requires a sputtering system equipped with a GDC target and a tube or box furnace. The most significant ongoing cost is for YSZ samples, which were $12.95 to $459.00 for sample areas ranging from 25 mm^2 to 2500 mm^2, respectively (MTI Corporation). However, if used for imprinting, samples could likely be employed repeatedly before replacement. Samples required ~4 hours of sputtering time and ~1-10 hours of annealing in a furnace to produce the final structures, all of which could be performed without supervision. Thus, the GDC/YSZ system provides a facile, economical alternative to lithographic processes for nanofeature manufacture. The primary disadvantage of this approach is that although regular features (Figures 1, 2) can be produced over large surface areas (mm^2) (Figures 3, 4), these features are randomly ordered (Figure 4); and therefore lithographic approaches may still be favored in applications where highly ordered features are required.

To demonstrate the potential of this system to influence cell attachment behavior, we examined the SK-N-SH neuroblastoma cell line, which is known to undergo morphological changes with culture density (11), on three nanofeature surfaces: islands, connected islands, and pits, and a smooth control surface. Of these surfaces, connected islands demonstrated more properties consistent with cell attachment (e.g., cell spreading,

polarization, and focal contact formation), whereas islands demonstrated the least. The most likely cause for this disparity is the size of the features. Islands display lower feature height and area, when compared to connected islands and pits surfaces (Table 1). Of these two, it is probable that feature area is the greater contributor because pits display similar feature heights to islands (albeit inverted in geometry), yet substantially improved cell attachment properties (e.g., Figures 5, 6).

Feature spacing most likely does not contribute as these are similar for both islands and connected islands surfaces (Table 1). It is interesting to note that whereas both connected islands and pits surfaces promoted cell polarization (Figure 7b), connected islands alone encouraged the best combination of cell attachment behaviors (Figure 7a, 8). Taken together, this data suggests that cell attachment is most strongly influenced by feature area, which was greatest for connected islands, followed by pits and islands (Table1). Decreased feature area may interfere with formation of focal contacts, preventing cell spreading and resulting in a circular morphology. It has been reported that features of 140 nm (i.e., 19,600 nm^2) are required for $\alpha_v\beta_3$-mediated focal contact formation and of 440 nm (i.e., 193,600 nm^2) are required for $\alpha_v\beta_3$-mediated cellular spreading (19). This report is confirmed by our results, in which SK-N-SH cells were observed to attach, but not spread on island surfaces, and exhibited limited spreading on pits surfaces.

This effect may also result in the lack of uniform cell morphology across the surface of the islands as islands dimensions vary across the substrate (Figure 5b).

A more unlikely possibility is that these discrepancies are produced by differing GDC concentration at the surface. Gadolinium can interfere with receptor function, for example inhibiting stretch activated channels (20, 21), and differences in surface

chemistry are likely as the surface reorders by diffusion of GDC and YSZ components. This is further supported by the observed differences in surface energy and contact angles among surfaces (Table 2). However, a gadolinium-influenced response is unlikely as spread cells were observed on connected islands, pits, and most importantly control surfaces, which present a uniform GDC surface, eliminating the possibility of GDC inhibition of stretch activated channels (20, 21).

It is also possible that differences in cell behavior result from alterations in protein adsorption, which would affect extracellular matrix deposition and ultimately cell adhesion. Preferential adsorption of certain proteins has been shown to change cell behavior in response to nanofeatures (22), and may play a role in this case. However, the similarities in contact angle and surface energy between connected islands and islands (69.0 and 64.6º, 42.34 and 45.01 mN/m, respectively), which display the most divergent cell attachment behaviors, do not support this conclusion. Thus, although it is possible that chemistry (i.e. GDC concentration or wettability) influences cell attachment behavior, it is far more likely that these differences result from nanotopography. Neuroblastoma cells have previously been shown to respond to the topography of nanogratings and nanocones (23, 24). However, no studies have been published on neural cell response to islands, connected islands, or pits of the same morphology utilized in this work. Much research has been performed on the response of fibroblast, endothelial, and epithelial cells to pits and islands of similar morphology produced by polymer demixing. These studies have shown increased cell spreading on islands ranging from 10 to 100 nm in height, in contrast to our observations. They have also shown decreased cytoskeletal organization in cells grown on islands of 34 and 95 nm islands, which is corroborated by

the results of our work (25). Other studies have shown increased adhesion to islands rather than pits, theorizing that finer features or larger island areas influence adhesion (26). This is also contradictory to our findings, in which we have found that pit morphologies provide similar cell spreading and adhesion to connected islands. However, it should be noted that our results suggest feature area, rather than height, may be a more important determinant of cell behavior in our system. Additionally, these discrepancies may result from differences in substrate chemistry or cell type.

The GDC/YSZ system thus provides many advantages for exploring the role of nanotopography in cell behavior. It is economical and can produce large-scale (mm^2) nanopatterned substrates whose *in vitro* results could be directly applied to implants at the same scale. It influences cell behavior, providing both adhesive (i.e., connected islands) and non-adhesive (i.e., islands) cues. The ceramic GDC/YSZ system is mechanically, thermally, and chemically stable (10), preventing degradation by proteolytic enzymes that can adversely affect surface patterning of active molecules (27). This durability and strength provides obvious potential application to orthopedic bone implants, which would require similar material properties to this ceramic system (28). However, we have also shown that these features can be imprinted into hydrogel substrates (Figure 9), enhancing applicability to soft tissue engineering. For example, we are currently exploring the potential of nanopatterned hydrogel surfaces to enhance corneal epithelial cell migration for treatment of eye injury. This capacity to imprint patterns into other substrates also provides great flexibility in material and chemical property selection that will permit controlled exploration of the role of topography vs. chemistry as fundamental manipulators in cell behavior. Thus, in addition to its potential

for clear and direct application to biomaterial implants and tissue engineering, GDC/YSZ substrates or their imprinted hydrogels could potentially be used as a model system to explore cell responses to nanotopography.

5. Overall Conclusions

The GDC/YSZ system provides an inexpensive, time efficient method of nanofabrication that significantly affects cell behavior. Nanopattern fabrication includes simple purchase of an YSZ substrate followed by sputter coating of a nanofilm of GDC and annealment in a tube or box furnace for 1-10 hours. There is no handling by the user except during the sputtering process which can be used to sputter coat a number of samples simultaneously. Furthermore, the system has additional advantages in that it can be scaled to the size of an oven and can produce multiple semi-ordered patterns, each spanning the entire surface of the substrate. Moreover, there is little additional cost or time associated with scaling up the size of the material. The sputtering and annealing steps are both equally time efficient for both small and large substrates and require the same amount of handling.

The GDC/YSZ system was validated through cell studies performed with SK-N-SH neuroblastoma cells. These cells showed immediate and significant changes in cell morphology and cell area based on whether they were seeded on island, connected island, or pit patterned surfaces. These changes from one patterned surface to another were further validated through cytoskeletal labeling studies depicting distinct changes in actin and vinculin formation upon each substrate. Additional studies further confirmed that topography did play a significant role in the modulation of neuroblastoma cell behavior. Contact angle measurements demonstrated similar surface chemistries for both the islands and connected islands; however, there were clear differences in cell morphology and cytoskeletal formation in cells grown on either substrate. This result clearly

illustrates that while chemistry may play a role in cell response to nanofeatures, topography on the nanoscale does have a significant effect.

The GDC/YSZ system has a number of unique properties that provide for its use in the development of biomaterials and in tissue engineering applications. In addition to its ability to produce multiple unique patterns, its unprecedented ease in scale-up, and its ability to significantly impact cell behavior, this system can also be imprinted into hydrogels providing material and chemical flexibility as well as direct *in vivo* application.

6. Recommendations for Future Direction

This work shows tremendous promise for use of the GDC/YSZ system in studying the effects of nanotopography on cell behavior as well as in the development of biomaterials. The system's unique qualities allow for facile production and scaling in addition to experimental flexibility in the development of multiple patterns on various surfaces. Current work focuses on utilizing the phenomenon of cell response to nanotopography to improve patient health in the development of a nanopatterned contact lens to accelerate corneal healing. The corneal epithelial basement membrane is also nanopatterned, and previous studies have shown that nanopatterned surfaces can not only orient cells and accelerate migration, but also increase cell proliferation (22). Thus, in the case of a corneal scratch, a nanopatterned lens may provide for accelerated wound healing by increasing proliferation and directing cells to the site of the injury. Additionally, this may allow for development of nanopatterned wound healing bandages, as the patterned epithelial layer is present throughout the body.

The GDC/YSZ system may also be utilized to further understanding of cellular response to nanopatterns. As mentioned previously, in order to truly utilize this phenomenon in the development of biomaterials, research must be conducted investigating the effect of multiple patterns at several dimensions and chemistries on a number of different cell types. Due to its facile and inexpensive manufacturing process, as well as its ability produce multiple patterns and be imprinted into hydrogels, the GDC/YSZ system may serve as the ideal basis for conducting this research. Furthermore, this controlled manner

of experimentation may also elucidate the mechanism behind changes in cell behavior when exposed to nanoscale features. To this day, there is little understanding of this intriguing process. Another experiment that could further illuminate this mechanism is the long term imaging of cytoskeletal proteins within cells utilizing quantum dots incorporated into the cell directly after passaging. In the past, organic dyes were used to observe how the cell's cytoskeleton had formed in response to nanopatterns, but this was done post cell attachment to the surface and was static in nature. The use of quantum dots to study how the cytoskeleton forms in response to different nanopatterns over a period of days may be enlightening.

Another area in which nanotopography is receiving more attention is in the controlled differentiation and culture of stem cells. These cells are extremely difficult to culture *in vitro*, precluding much needed experimentation and analysis by scientists. The GDC/YSZ system may be able to better mimic the *in vivo* environment and allow for culture of these important cell types. Furthermore, because of its ability to combine nanotopography with different material and chemical characteristics (via imprinting into hydrogels), this system may also serve to further understanding of the stem cell niche.

Bibliography

1. Curtis, A. and M. Riehle. Tissue Engineering: the Biophysical Background. Physics in Medicine and Biology. 2001;46:R47-R65.

2. Harrison RG. On the Stereotropism of embryonic cells. Science. 1911;34:279-81.

3. Curtis ASG, Varde M. Control of Cell Behavior: Topological factors. Journal of the National Cancer Research Institute. 1964;33:15-26.

4. Curtis ASG, Wilkinson CDW. Reactions of Cells to Topography. Journal of Biomaterial Science Polymer Edition. 1998;9(12):1313-29.

5. Chen Y, Pepin A. Nanofabrication: conventional and nonconventional methods. Electrophoresis. 2001;22:187-207.

6. Baac H, Lee H, Seo J, Park TH, Chung H, Lee S, et al. Submicron-scale topographical control of cell growth using holographic surface relief grating. Materials Science and Engineering C. 2004;24:209-12.

7. Norman JJ, Desai TA. Methods for Fabrication of Nanoscale Topography for Tissue Engineering Scaffolds. Annals of Biomedical Engineering. 2006;34(1):89-101.

8. Wu W, Dey D, Memis OG, Katsnelson A, Mohseni H. Fabrication of large area periodic nanostructures using nanosphere photolithography. Nanoscale Research Letters. 2008 Oct;3(10):351-4.

9. Rauscher MD, Boyne A, Dregia SA, Akbar SA. Self-Assembly of Pseudoperiodic Arrays of Nanoislands on YSZ-(001). Advanced Materials. 2008;20:1699-705.

10. Zimmerman LB, Rauscher MD, Ellis J, Boukany P, Lee LJ. Nanoimprinting using self-assembled ceramic nanoislands. Nanotechnology. 2010;21:1-6.

11. Biedler JL, Helson L, Spengler BA. Morphology and Growth, Tumorigenicity, and Cytogenetics of Human Neuroblastoma Cells in Continuous Culture. Cancer Research. 1973;33:2643-52.

12. Li D, Neumann AW. Equation of State for Interfacial Tensions of Solid-Liquid Systems. Advances in Colloid and Interface Science. 1992;39:299-345.

13. http://www.kruss.de/en/theory/measurements/contact-angle/models/equation-of-state.html. [cited 2011 November 21].

14. Lim JY, Hansen JC, Siedlecki CA, Runt J, Donahue HJ. Human foetal osteoblastic cell response to polymer-demixed nanotopographic interfaces. Journal of the Royal Society Interface. 2005;2(2):97-108.

15. Winter JO, Liu TY, Korgel BA, Schmidt CE. Recognition Molecule Directed Interfacing Between Semiconductor Quantum Dots and Nerve Cells. Advanced Materials. 2001;13(22):1673-7.

16. Peppas NA. Hydrogels. In: Ratner BD, Hoffman AS, Schoen FJ, Lemons JE, editors. Biomaterials Science: An Introduction to Materials in Medicine. 2nd Ed. ed. London: Elsevier; 2004. p. 100-7.

17. Lin CC, Anseth KS. PEG Hydrogels for the Controlled Release of Biomolecules in Regenerative Medicine. Pharm Res. [Review]. 2009 Mar;26(3):631-43.

18. Tessmar JK, Gopferich AM. Customized PEG-derived copolymers for tissue-engineering applications. Macromol Biosci. 2007 Jan 5;7(1):23-39.

19. Massia SP, Hubbell JA. An RGD Spacing of 440 nm Is Sufficient for Integrin avß3-mediated Fibroblast Spreading and 140 nm for Focal Contact and Stress Fiber Formation. Journal of Cell Biology. 1991;114(5):1089-100.

20. Naruse K, Sai X, Yokoyama N, Sokabe M. Uni-axial cyclic stretch induces c-src activation and translocation in human endothelial cells via SA channel activation. FEBS Lettters. 1998;441:111-5.

21. Robson L, Hunter M. Volume-activated, gadolinium-sensitive whole-cell currents in single proximal cells of frog kidney. Pflugers Archive European Journal of Physiology. 1994;429:98-106.

22. Texeira AI, Abrams GA, Bertics PJ, Murphy CJ, Nealey PF. Epithelial contact guidance on well-defined micro- and nanostructured substrates. Journal of Cell Science. 2003;116:1881-92.

23. Bettinger CJ, Langer R, Borenstein JT. Engineering Substrate Topography at the Micro-and Nanoscale to Control Cell Function. Angewandte Chemie International Edition. 2009;48:2-12.

24. Purwaningsih L, Schoen T, Wolfram T, Pacholski C, Spatz JP. Fabrication of multi-parametric platforms based on nanocone arrays for determination of cellular response. Beilstein J Nanotechnol. 2011;2:545-51.

25. Dalby MJ, Pasqui D, Affrossman S. Cell response to nano-islands produced by polymer demixing: a brief review. IEE Proceedings: Nanobiotechnology. 004;151(2):53-61.

26. Lim JY, Hansen JC, Siedlecki CA, Hengstebeck RW, Cheng J, Winograd N, et al. Osteoblast Adhesion on Poly(L-lactic Acid)/Polystyrene Demixed Thin Film Blends:

Effect of Nanotopography, Surface Chemistry, and Wettability. Biomacromolecules. 2005;6:3319-27.

27. Wilkinson CDW, Riehle M, Wood M, Gallagher J, Curtis ASG. The use of materials patterned on a nano- and micro-metric scale in cellular engineering. Materials Science and Engineering C. 2002;19:263-9.

28. Biggs MJP, Richards RG, Gadegaard N, McMurray RJ, Affrossman S, Wilkinson CDW, et al. Interactions with nanoscale topography: Adhesion, quantification, and signal transduction in cells of osteogenic and multipotent lineage. J Biomed Mater Res. 2008;91A:195-208.